J|A|C|S
ARTICLES
Published on Web 08/23/2007

Rapid Three-Step Cleavage of RNA and DNA Model Systems Promoted by a Dinuclear Cu(II) Complex in Methanol. Energetic Origins of the Catalytic Efficacy

Zhong-Lin Lu,† C. Tony Liu, Alexei A. Neverov, and R. Stan Brown*

Contribution from the Department of Chemistry, Queen's University, Kingston, Ontario, Canada, K7L 3N6

Received June 4, 2007; E-mail: rsbrown@chem.queensu.ca

Abstract: A dinuclear Cu(II) complex of 1,3-*bis*-N_1-(1,5,9-triazacyclododecyl)propane with an associated methoxide (**2**-Cu(II)$_2$:($^-$OCH$_3$)) was prepared, and its kinetics of reaction with an RNA model (2-hydroxypropyl-*p*-nitrophenyl phosphate (**1**, HPNPP)) and two DNA models (methyl *p*-nitrophenyl phosphate (**3**) and *iso*-butyl *p*-chlorophenyl phosphate (**4**)) were studied in methanol solution at ^s_spH 7.2 ± 0.2. X-ray diffraction structures of **2**-Cu(II)$_2$:($^-$OH)(H$_2$O)(CF$_3$SO$_3^-$)$_3$:0.5CH$_3$CH$_2$OCH$_2$CH$_3$ and **2**-Cu(II)$_2$:($^-$OH)((C$_6$H$_5$-CH$_2$O)$_2$PO$_2^-$)(CF$_3$SO$_3^-$)$_2$ show the mode of coordination of the bridging $^-$OH and H$_2$O between the two Cu(II) ions in the first complex and bridging $^-$OH and phosphate groups in the second. The kinetic studies with **1** and **3** reveal some common preliminary steps prior to the chemical one of the catalyzed formation of *p*-nitrophenol. With **3**, and also with the far less reactive substrate (**4**), two relatively fast events are cleanly observed via stopped-flow kinetics. The first of these is interpreted as a binding step which is linearly dependent on [catalyst] while the second is a unimolecular step independent of [catalyst] proposed to be a rearrangement that forms a doubly Cu(II)-coordinated phosphate. The catalysis of the cleavage of **1** and **3** is very strong, the first-order rate constants for formation of *p*-nitrophenol from the complex being ~0.7 s^{-1} and 2.4×10^{-3} s^{-1}, respectively. With substrate **3**, **2**-Cu(II)$_2$:($^-$OCH$_3$) exhibits Michaelis−Mentin kinetics with a k_{cat}/K_M value of 30 M^{-1} s^{-1} which is 3.8×10^7-fold greater than the methoxide promoted reaction of **3** (7.9×10^{-7} M^{-1} s^{-1}). A free energy calculation indicates that the binding of **2**-Cu(II)$_2$:($^-$OCH$_3$) to the transition states for **1** and **3** cleavage stabilizes them by −21 and −24 kcal/mol, respectively, relative to that of the methoxide promoted reactions. The results are compared with a literature example where the cleavage of **1** in water is promoted by a dinuclear Zn(II) catalyst, and the energetic origins of the exalted catalysis of the **2**-Cu(II)$_2$ and **2**-Zn(II)$_2$ methanol systems are discussed.

1. Introduction

Phosphodiesters are important biomolecules for the storage of genetic information due to their great stability.[1−7] The half-times for hydrolysis of RNA[8] and DNA[9] at pH 7 and 25 °C are reported to be 110 and up to 100 billion years, respectively. Certain phosphodiesterase enzymes promote the cleavage by up to a factor of 10^{15-16} giving some of the most spectacular rate enhancements known. Many of these contain active sites with two or more metal ions (usually Zn^{2+} and in some cases Mg^{2+}, Ca^{2+}, and Fe^{2+}) as exemplified by ribonuclease H from HIV reverse transcriptase,[5] 3′,5′-exonuclease from DNA polymerase I,[6] the P1 nucleases,[7] and phospholipase C.[1−4] Not surprisingly, intense research is directed at understanding the origins of catalysis of phosphate diester cleavage provided by metal ion containing systems.[10−13] The earlier work[10−13] and more recent reports[14−20] indicate that dinuclear complexes are typically more reactive than their mononuclear counterparts, although in some cases they are slower or only weakly accelerating.[18,21,22] Very recently we reported on the exalted

† Presently at Beijing Normal University, College of Chemistry, Beijing, China, 100875.

(1) Weston, J. *Chem. Rev.* **2005**, *105*, 2151.
(2) Cowan, J. A. *Chem. Rev.* **1998**, *98*, 1067.
(3) Wilcox, D. E. *Chem. Rev.* **1996**, *96*, 2435.
(4) Sträter, N.; Lipscomb, W. N.; Klabunde, T.; Krebs, B. *Angew. Chem., Int. Ed. Engl.* **1996**, *35*, 2024.
(5) Davies, J. F.; Hostomska, Z.; Hostomsky, Z.; Jordan, S. R.; Mathews, D. A. *Science* **1991**, *252*, 88.
(6) Beese, L. S.; Steitz, T. A. *EMBO J.* **1991**, *10*, 25.
(7) Lahm, A.; Volbeda, S.; Suck, D. *J. Mol. Biol.* **1990**, *215*, 207.
(8) Schroeder, G. K.; Lad, C.; Wyman, P.; Williams, N. H.; Wolfenden, R. *Proc. Natl. Acad. Sci. U.S.A.* **2006**, *103*, 4052.
(9) Williams, N. H.; Wyman, P. *Chem. Commun.* **2001**, 1268.
(10) Molenveld, P.; Engbertsen, J. F. J.; Reinhoudt, D. N. *Chem. Soc. Rev.* **2000**, *29*, 75.
(11) Williams, N. H.; Takasaki, B.; Wall, M.; Chin, J. *Acc. Chem. Res.* **1999**, *32*, 485.
(12) Mancin, F.; Scrimin, P.; Tecilla, P.; Tonellato, U. *Chem. Commun.* **2005**, 2540.
(13) Morrow, J. R.; Iranzo, O. *Curr. Opin. Chem. Biol.* **2004**, *8*, 192.
(14) Yamada, K.; Takahashi, Y.-i.; Yamamura, H.; Araki, A.; Saito, K.; Kawai, M. *Chem. Commun.* **2000**, 1315.
(15) Feng, G.; Mareque-Rivas, J. C.; Williams, N. H. *Chem. Commun.* **2006**, 1845.
(16) Mancin, F.; Rampazzo, E.; Tecilla, P.; Tonellato, U. *Eur. J. Chem.* **2004**, 281.
(17) Yang, M.-Y.; Iranzo, O.; Richard, J. P.; Morrow, J. R. *J. Am. Chem. Soc.* **2005**, *127*, 1064.
(18) Iranzo, O.; Elmer, T.; Richard, J. P.; Morrow, J. R. *Inorg. Chem.* **2003**, *42*, 7737.
(19) Iranzo, O.; Richard, J. P.; Morrow, J. R. *Inorg. Chem.* **2004**, *43*, 1743.
(20) Iranzo, O.; Kovalevsky, A. Y.; Morrow, J. R.; Richard, J. P. *J. Am. Chem. Soc.* **2003**, *125*, 1988.
(21) Bauer-Sienbenlist, B.; Meyer, F.; Farkas, E.; Vidovic, D.; Cuesta-Seijo, J. A.; Herbst-Irmer, R.; Pritzkow, H. *Inorg. Chem.* **2004**, *43*, 4189.

10.1021/ja073780l CCC: $37.00

Scheme 1 [a]

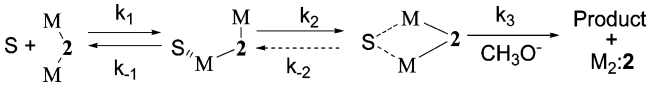

[a] M = Zn(II) or Cu(II), S = phosphodiester substrate; charges omitted for simplicity.

catalysis of the cleavage of an RNA model, 2-hydroxypropyl *p*-nitrophenyl phosphate (HPNPP (**1**)), promoted by a dinuclear Zn^{2+} complex (**2**-Zn(II)$_2$) in methanol.[23] The plot of k_{obsd} for the process vs [**2**-Zn(II)$_2$] in the presence of 1 equiv of added methoxide (which attaches to the metal ions to form **2**-Zn(II)$_2$:($^-$OCH$_3$) and maintains the ^s_spH[24] at 9.5−9.8) was linear with a slope of $k_2^{obsd} = 275\,000\ M^{-1}\ s^{-1}$. This catalytic k_2^{obsd} value is 10^8 larger than the methoxide promoted cyclization of **1** ($2.56 \times 10^{-3}\ M^{-1}\ s^{-1}$)[23] and far exceeds anything previously seen in water. A similar plot for the methanolysis of a DNA model (methyl *p*-nitrophenyl phosphate (MNPP (**3**)) exhibits Michaelis−Mentin behavior with K_M and k_{max} values of 0.37 ± 0.07 mM and $(4.1 \pm 0.3) \times 10^{-2}\ s^{-1}$. That two closely related substrates exhibit such different kinetic behaviors seemed unusual and was rationalized by invoking the mechanism given in Scheme 1 where the rate-limiting step with **1** was its binding (k_1 or k_2) while that with the slower reacting **3** was the chemical step of methanolysis of the bound substrate (k_3).

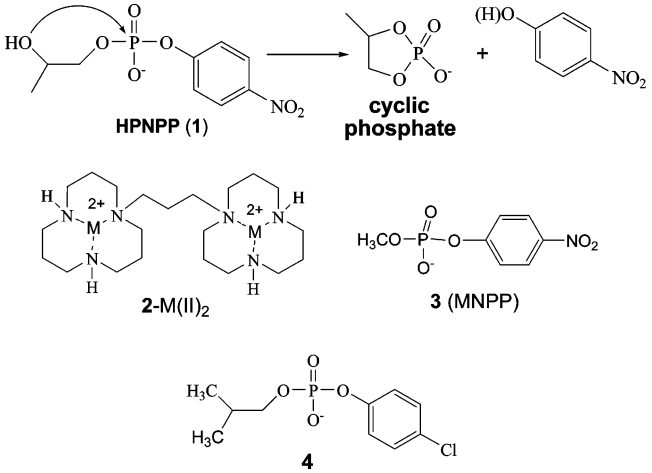

Herein we present results with the Cu(II)$_2$ complex of **2** that supports the above mechanism. While it is true that Cu(II) complexes prefer five- and six-coordinate environments which are different from Zn(II) complexes, several of the former are known to catalyze phosphoryl transfer reactions of phosphate diesters and interesting information of relevance to the mechanism of action has been obtained from their study.[16,22,25−29] Unlike Zn(II) complexes, those with Cu(II) are also highly colored which can give information about changes in the immediate coordination environment around the metal ion. As will be shown, the **2**-Cu(II)$_2$ complex greatly catalyzes the cleavages of both **1** and **3**, and it also exhibits two clearly defined steps confirmed with **3** and diester **4** which appear to be associated with the binding of these substrates to **2**-Cu(II)$_2$.

2. Experimental Section

2.1. Materials. Methanol (99.8% anhydrous), sodium methoxide (0.5 M) solution in methanol, dibenzyl phosphate, and Cu(CF$_3$SO$_3$)$_2$ were purchased and used without further purification. Methyl-*p*-nitrophenyl phosphate (MNPP, **3**) was prepared according to a general published method[30] while 2-methylpropyl *p*-chlorophenyl phosphate (MPClPP, **4**) was prepared as described in the Supporting Information. 1,3-Bis-N$_1$-(1,5,9-triazacyclododecyl)propane (**2**) was synthesized according to the published procedure.[31] The sodium salt of 2-hydroxylpropyl *p*-nitrophenyl phosphate (**1**) was prepared according to the literature procedure[32] with a slight modification.[33] The dinuclear complex (**2**-Cu(II)$_2$:($^-$OCH$_3$)) was prepared as a 2.5 mM solution in methanol by sequential addition of aliquots of stock solutions of sodium methoxide, 1,3-bis-N$_1$-(1,5,9-triazacyclododecyl)propane,[31] and Cu(CF$_3$SO$_3$)$_2$ in relative amounts of 1:1:2. *It has been found that this order of addition is essential for the formation of the complex, and even then its complete formation is achieved only after 10−15 min (as monitored by the increase in catalytic activity as a function of time).*

2.2. Methods. ^{1}H NMR and ^{31}P NMR spectra were determined at 400 and 162.04 MHz. The CH$_3$OH$_2^+$ concentration was determined using a combination of glass electrode (Radiometer model no. XC100-111-120-161) calibrated with standard aqueous buffers (pH = 4.00 and 10.00) as described in previous papers.[23,33] The ^s_spH values in methanol[34] were determined by subtracting a correction constant of −2.24 from the readings obtained from the electrode, while the autoprotolysis constant was taken to be $10^{-16.77}$. The ^s_spH values for the kinetic experiments were simply measured from solutions of the complexes which were made *in situ* by the addition of 1 equiv of ligand **2**, 1 equiv of NaOCH$_3$, and 2 equiv of Cu(OTf)$_2$: the values determined in this manner lie in the region 7.0−7.6, but mostly at 7.2−7.4 for the concentrations where the catalysis was investigated. While the methodology gives some variance in the measured ^s_spH values particularly at low concentrations of metal ion, we have found that the addition of buffers to control the ^s_spH retards the reaction probably due to inhibition by the associated counterions binding to the catalyst. The first and second ^s_sp$K_a$values for **2**-Cu(II)$_2$:(HOCH$_3$) (0.4 mM) were determined from duplicate measurements to be 6.77 ± 0.01 and 7.82 ± 0.03 by measuring the ^s_spH at half neutralization whereby the [**2**-Cu(II)$_2$:($^-$OCH$_3$)]/[**2**-Cu(II)$_2$:(HOCH$_3$)] or [**2**-Cu(II)$_2$:($^-$OCH$_3$)$_2$]/[**2**-Cu(II)$_2$:($^-$OCH$_3$)] ratios were 1.0. This involved treating **2**-Cu(II)$_2$:($^-$OCH$_3$), prepared as described above at 0.4 mM, with 0.5 equiv of 70% HClO$_4$ or NaOCH$_3$ diluted to a 0.05 M stock solution in anhydrous methanol and measuring the ^s_spH.

2.3. Kinetics. The rates of cleavage of MNPP (**3**) (0.04 mM) catalyzed by **2**-Cu(II)$_2$:($^-$OCH$_3$) (5×10^{-5} to 6×10^{-4} M) were followed by monitoring the appearance of *p*-nitrophenol at 320 nm at 25.0 ± 0.1 °C. The fast rates of binding steps of substrates **1**, **3**, and **4** (0.03 mM) to **2**-Cu(II)$_2$:($^-$OCH$_3$) in anhydrous methanol were followed by observing the changes in the Cu(II)$_2$ band at 340 nm at 25 °C using a stopped-flow reaction analyzer with a 10 mm light path.

(22) Arca, M.; Bencini, A.; Berni, E.; Caltagiirone, C.; Devillanova, F. A.; Isaia, F.; Garau, A.; Giorgi, C.; Lippolis, V.; Perra, A.; Tei, L.; Valtancoli, B. *Inorg. Chem.* **2003**, *42*, 6929.
(23) Neverov, A. A.; Lu, Z. L.; Maxwell, C. I.; Mohamed, M. F.; White, C. J.; Tsang. J. S. W.; Brown, R. S. *J. Am. Chem. Soc.* **2006**, *128*, 16398.
(24) For the designation of pH in nonaqueous solvents we use the forms recommended by the IUPAC, *Compendium of Analytical Nomenclature. Definitive Rules 1997*, 3rd ed.; Blackwell: Oxford, U.K., 1998. Since the autoprotolysis constant of methanol is $10^{-16.77}$, neutral ^s_spH is 8.4.
(25) Rossi, L. M.; Neves, A.; Hörner, R.; Terenzi, H.; Szpoganicz, B.; Sugai, J. *Inorg. Chim. Acta* **2002**, *337*, 366.
(26) Deal, K. A.; Hengge, A. C.; Burstyn, J. N. *J. Am. Chem. Soc.* **1996**, *118*, 1713.
(27) Jagoda, M.; Warzeska, S.; Pritzkow, H.; Wadepohl, H.; Imhof, P.; Smith, J. C.; Krämer, R. *J. Am. Chem. Soc.* **2005**, *127*, 15061.
(28) Fry, F. H.; Fischmann, A. J.; Belousoff, M. J.; Spiccia, L.; Brügger, J. *Inorg. Chem.* **2005**, *44*, 941 and references therein.
(29) Deal, K. A.; Park, G.; Shao, J.; Chasteen, N. D.; Brechbiel, M. W.; Planalp, R. P. *Inorg. Chem.* **2001**, *40*, 4176.
(30) Kirby, A. J.; Younas, M. *J. Chem. Soc. B* **1970**, 1165.
(31) Kim, J.; Lim, H. *Bull. Korean Chem. Soc.* **1999**, *20*, 491.
(32) Brown, D. M.; Usher, D. A. *J. Chem. Soc.* **1965**, 6558.
(33) Tsang, J. S.; Neverov, A. A.; Brown, R. S. *J. Am. Chem. Soc.* **2003**, *125*, 1559.
(34) Gibson, G.; Neverov, A. A.; Brown, R. S. *Can. J. Chem.* **2003**, *81*, 495.

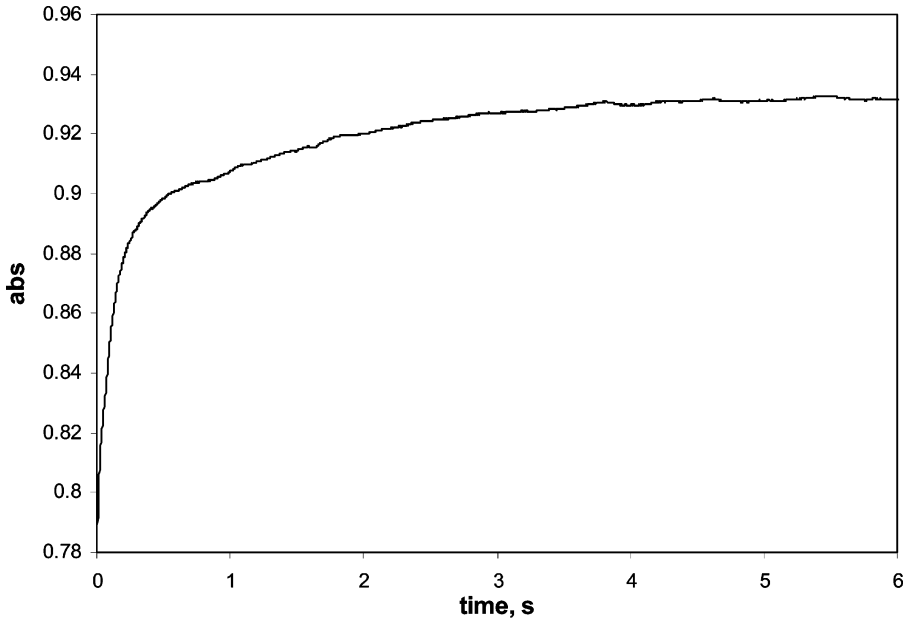

Figure 1. Absorbance vs time profile for the reaction of 0.5 mM **2**-Cu(II)$_2$:($^-$OCH$_3$) and 0.03 mM **1** in methanol, ^s_spH = 7.4, followed at 340 nm.

In the case of **1**, the second binding step is superimposed on that for the production of *p*-nitrophenol which leads to a rise in absorbance as shown in Figure 1. For the sets of experiments with **1** and **3** the [**2**-Cu(II)$_2$:($^-$OCH$_3$)] was varied from 0.25 to 1.0 mM. The two fast steps (termed herein as the first and second binding events) for **4** (0.03 mM) were followed at 340 and 380 nm also using stopped-flow spectrophotometry at 25 °C with the [**2**-Cu(II)$_2$:($^-$OCH$_3$)] being varied from 0.4 to 1.0 mM. The first-order rate constants (k_{obsd}) for first and second events with all substrates were obtained by fitting the UV/vis absorbance vs time traces to a standard biexponential model. The second-order rate constants for the first binding event (k_1) for each substrate were determined from the slopes of k_{obsd} vs [**2**-Cu(II)$_2$:($^-$OCH$_3$)] plots, while the second binding event for each was found to be independent of the [**2**-Cu(II)$_2$:($^-$OCH$_3$)] and is simply referred to as k_2. Given in Table 2 are the rate constants with the original data being given in Tables 1S−7S of the Supporting Information.

2.4. Mass Spectra. The methanolysis of 0.5 mM of MNPP by 0.5 mM of catalyst was also monitored by ESI mass spectroscopy with the following conditions: ESI+ mode, declustering potential = 80.0 V, N_2 carrier gas, ion spray voltage = 5500 V, resolution = 10 000, and direct syringe injection. The reaction progress was followed by comparing the relative ratio of the sums of the integrated intensities of all product species, or all the substrate species in solution vs the sums of the integrated intensities of all product and substrate species in solution (respectively, **2**-Cu(II)$_2$:(X^-)(Y^-)(($CH_3O)_2PO_2^-$) or **2**-Cu(II)$_2$:(X^-)(Y^-)(($NO_2C_6H_4O$)(CH_3O)PO_2^-), where X^- and Y^- = $CF_3SO_3^-$, **3** or $(CH_3O)_2PO_2^-$. MS spectra were taken at time = 0.7, 3.7, 13.7, 22.7, 42.7, and 116.7 min, and aliquots were removed from the reaction mixture by syringe and manually injected. Representative examples of the spectra are given in the Supporting Information.

2.5. X-ray Diffraction. The crystal structures of **2**-Cu(II)$_2$:($^-$OH)(H_2O)($CF_3SO_3^-$)$_3$ and **2**-Cu(II)$_2$:($^-$OH)(($C_6H_5CH_2O)_2PO_2^-$)($CF_3SO_3^-$)$_2$ were determined using a Bruker SMART APEX II X-ray diffractometer with graphite-monochromated Mo Kα radiation (λ = 0.710 73 Å), operating at 50 kV and 30 mA over 2θ ranges of 3.86°−50.00° as described in the Supporting Information. No significant decay was observed during the data collection at −93 °C. Crystals of **2**-Cu(II)$_2$:($^-$OH)(H_2O)($CF_3SO_3^-$)$_3$:0.5 $CH_3CH_2OCH_2CH_3$ suitable for study were grown from a methanol solution containing 1 equiv each of **2** and $NaOCH_3$ along with 2 equiv of Cu(OTf)$_2$ placed in the lower chamber of a necked-down sealed tube, which was gently overlaid with an ether layer which was allowed to diffuse into the methanolic solution over 4 days. Crystals of **2**-Cu(II)$_2$:($^-$OH)(($C_6H_5CH_2O)_2PO_2^-$)($CF_3SO_3^-$)$_2$ were grown from a methanol solution containing 1 equiv each of **2**, $NaOCH_3$ and the sodium salt of dibenzyl phosphate along with 2 equiv of Cu(OTf)$_2$. The methanol solution was allowed to evaporate slowly over 4 days without protection from the atmosphere at ambient temperature. Given in Table 1 are crystal data and structural refinement details. The ORTEP diagrams at the 50% probability level for each of the two complexes are given in Figure 7. Full structural details and CIF files for each complex are given in the Supporting Information.

3. Results

Given in Figure 1 is the Abs vs time profile for the methanolysis of 0.03 mM **1** promoted by 0.5 mM **2**-Cu(II):($^-$OCH$_3$) (^s_spH = 7.4) determined at 340 nm. The trace is clearly biphasic indicating at least two events. The absorbance vs time data were fit by NLLSQ to a standard biexponential model for an A → B → C process under the assumption that the absorbance change for the second step was constant and controlled by the appearance of *p*-nitrophenol with a fixed ΔA_2 of 0.05 abs units. The first-order rate constants for the first and second events are 10.4 s^{-1} and 0.72 s^{-1}.

Shown in Figure 2a and 2b are the plots of the first-order rate constants for the first and second events observed for the methanolysis of 0.03 M HPNPP obtained under pseudo-first-order conditions of excess catalyst concentration, 0.25 mM < [**2**-Cu(II):($^-$OCH$_3$)] < 1.0 mM, ^s_spH = 7.4 ± 0.2. The second-order rate constant for the first event (k_1), calculated as the linear regression of the line, is 18 000 ± 700 M^{-1} s^{-1}, and at the 95% confidence level, the rate constant (k_2) for the second event is not dependent on the [**2**-Cu(II)$_2$:($^-$OCH$_3$)], the average value being 0.7 s^{-1}.

To probe further the origins of the first and second events, we switched to the DNA model, **3**, which does not possess the intramolecular 2-hydroxypropyl group and for which the release of *p*-nitrophenol is slower than that from **1** by a factor of at least 3200-fold for the methoxide catalyzed process.[33,35] Shown

(35) The second-order rate constant for methoxide catalyzed methanolysis of **3** is $k_2^{OMe^-}$ = (7.9 ± 0.6) × 10^{-7} M^{-1} s^{-1} (see ref 23), while that for reaction with **1** is 2.6 × 10^{-3} M^{-1} s^{-1}.

Table 1. Crystal Data and Structural Refinement Details for Crystals of **2**-Cu(II)$_2$:($^-$OH)(H$_2$O)(CF$_3$SO$_3^-$)$_3$·0.5Et$_2$O and **2**-Cu(II)$_2$:($^-$OH)((C$_6$H$_5$CH$_2$O)$_2$PO$_2^-$)(CF$_3$SO$_3^-$)$_2$

identification code	**2**-Cu(II)$_2$:($^-$OH)(H$_2$O)(CF$_3$SO$_3^-$)$_3$	**2**-Cu(II)$_2$:($^-$OH)((C$_6$H$_5$CH$_2$O)$_2$PO$_2^-$)(CF$_3$SO$_3^-$)$_2$
empirical formula	$C_{26}H_{54}Cu_2F_9N_6O_{11.50}S_3$; $[Cu_2(OH)(OH_2)(C_{21}H_{46}N_6)](CF_3SO_3)_3 \cdot 0.5Et_2O$	$C_{37}H_{59}Cu_2F_6N_6O_{11}\,P\,S_2$
formula weight	1029.01	1100.07
temperature	180(2) K	180(2) K
wavelength	0.710 73 Å	0.710 73 Å
crystal system	monoclinic	triclinic
space group	*C*2/*m*	
unit cell dimensions	$a = 17.647(4)$ Å $\alpha = 90°$ $b = 14.230(3)$ Å $\beta = 96.196(5)°$ $c = 16.367(4)$ Å $\gamma = 90°$	$a = 11.8724(16)$ Å $\alpha = 77.490(2)°$ $b = 14.0342(17)$ Å $\beta = 70.893(3)°$ $c = 15.446(2)$ Å $\gamma = 73.312(3)°$
volume	4086.1(16) Å^3	2307.9(5) Å^3
Z	4	2
density (calculated)	1.673 Mg/m^3	1.583 Mg/m^3
absorption coefficient	1.296 mm^{-1}	1.134 mm^{-1}
F(000)	2124	1140
crystal size	0.25 × 0.08 × 0.06 mm^3	0.30 × 0.20 × 0.20 mm^3
theta range for data collection	1.84° to 25.00°	1.93° to 25.00°
index ranges	$-19 \le h \le 20$, $-15 \le k \le 16$, $-19 \le l \le 19$	$-13 \le h \le 14$, $-16 \le k \le 16$, $0 \le l \le 18$
reflections collected	12 177	15 311
independent reflections	3760 [*R*(int) = 0.1045]	15 333 [*R*(int) = 0.0000]
completeness to $\theta = 25.00°$	99.7%	99.5%
absorption correction	empirical	TWINABS
max and min transmission	0.3183 and 0.1805	0.8050 and 0.7273
refinement method	full-matrix least-squares on F^2	full-matrix least-squares on F^2
data/restraints/parameters	3760/3/324	15 333/0/591
goodness-of-fit on F^2	1.000	1.000
final *R* indices [$I > 2\sigma(I)$]	R1 = 0.0830, wR2 = 0.2244	R1 = 0.0519, wR2 = 0.1385
R indices (all data)	R1 = 0.1371, wR2 = 0.2526	R1 = 0.0749, wR2 = 0.1483
largest diff peak and hole	0.997 and −1.195 e·Å^{-3}	0.722 and −0.592 e·Å^{-3}

in Figure 3 is a plot of the k_{obsd} vs varying [**2**-Cu(II)$_2$:($^-$OCH$_3$)] where the rate of formation of the *p*-nitrophenol product was followed at 320 nm by conventional UV/vis kinetics. The plot shows Michaelis−Mentin behavior with strong binding. The data for this can be fit to a universal binding equation, eq 1,[36] that is applicable to both strong and weak binding situations:

$$k_{obsd} = k_{cat}(1 + K_d*[Lim] + [Ex]*K_d - X)/(2K_d)/[Lim] \quad (1)$$

where [Lim] and [Ex] refer to total concentrations of limiting and excess reagents and X is given in eq 2.

$$X = (1 + 2K_d*[Lim] + 2*[Ex]*K_d + K_d{}^2*[Lim]^2 - 2*K_d{}^2*[Ex][Lim] + [Ex]^2*K_d{}^2)^{0.5} \quad (2)$$

NLLSQ fitting of the data to eqs 1, 2 gives a K_M of 0.079 ± 0.018 mM and a k_{cat} for the fully bound substrate of (2.40 ± 0.04) × 10^{-3} s^{-1}.

When the absorbance vs time profile for the methanolysis of **3** promoted by **2**-Cu(II)$_2$:($^-$OCH$_3$) is monitored at 320−340 nm on the stopped-flow time scale, there is evidence for three events, with two rapid events coming before the one relating to the release of *p*-nitrophenol from the bound substrate. Shown in Figure 4 are traces for the methanolysis of 0.05 mM **3** promoted by 0.5 mM **2**-Cu(II)$_2$:($^-$OCH$_3$) observed at $\lambda = 340$ (for the first two steps) and 320 nm (for the final step) and ^s_spH = 7.1 emphasizing the three temporally well-separated events with rate constants of 2.4 s^{-1}, 0.57 s^{-1}, and 2.10 × 10^{-3} s^{-1}.

The absorbance vs time traces for the first two steps of the reaction of **3** were monitored at 340 nm as a function of varying [catalyst], 0.25 mM < [**2**-Cu(II):($^-$OCH$_3$)] < 1.0 mM, ^s_spH = 7.2 ± 0.2. The first step is linear in [catalyst] (k_1 = 20 200 ± 600 M^{-1} s^{-1}), but the second step is independent of [**2**-Cu(II)$_2$:($^-$OCH$_3$)], the average value for k_2 being 0.53 ± 0.06 s^{-1} (see Table 2 and Supporting Information).

The methanolysis reaction of 5 × 10^{-4} M each of **3** and **2**-Cu(II)$_2$:($^-$OCH$_3$), in anhydrous methanol, was monitored by electrospray mass spectrometry at various times after mixing of the two components. The integrated intensities of all major peaks containing the methanolysis product (dimethyl phosphate) or substrate (**3**) bound to **2**-Cu(II)$_2$ along with any counterions present (e.g., respectively, **2**-Cu(II)$_2$:(X$^-$)(Y$^-$)((CH$_3$O)$_2$PO$_2^-$) or **2**-Cu(II)$_2$:(X$^-$)(Y$^-$)((NO$_2$C$_6$H$_4$O)(CH$_3$O)PO$_2^-$, X$^-$, Y$^-$ = triflate, **3**, or product) were summed to obtain ($I_{prod} + I_3$). The reaction progress was monitored by observing the $I_{prod}/(I_{prod} + I_3)$ and $I_3/(I_{prod} + I_3)$ ratios as a function of time (0.7, 3.7, 13.7, 22.7, 42.7, and 116.7 min). Figure 5 displays the results from which one can calculate the first-order rate constants of k_{prod} = 0.031 ± 0.007 min^{-1} and k_3 = 0.022 ± 0.003 min^{-1}.

(36) Equation 1 was obtained from the equations for equilibrium binding and for conservation of mass by using the commercially available MAPLE software, *Maple V*, release 5; Waterloo Maple Inc.: Waterloo, Ontario, Canada.

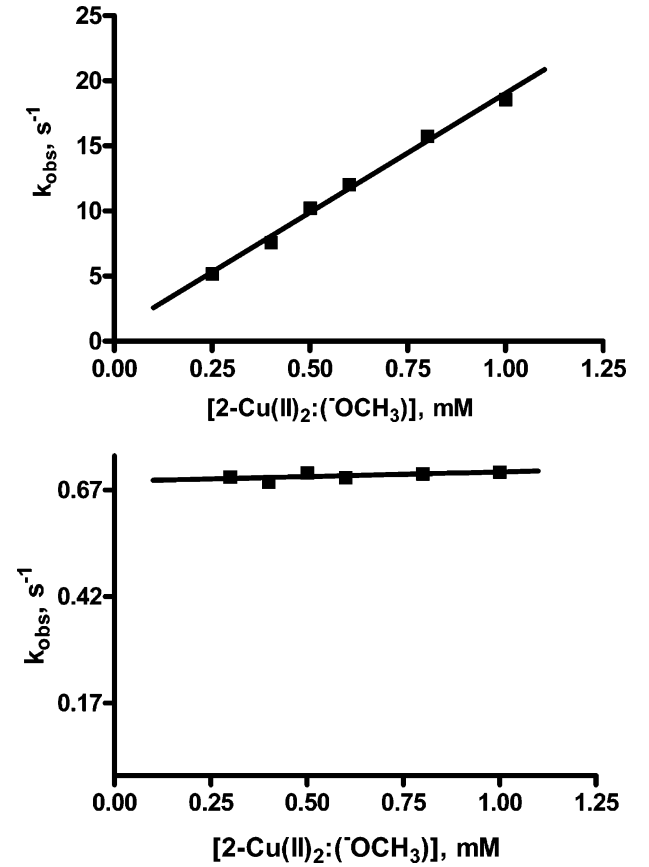

Figure 2. (Top) A plot of k_{obsd} vs [**2**-Cu(II)$_2$:($^-$OCH$_3$)] for the first event with NaHPNPP (3×10^{-5} M) at 340 nm in anhydrous methanol. The gradient of the line is 18 000 ± 700 M^{-1} s^{-1}, ^s_spH = 7.4 ± 0.2. (Bottom) A plot of k_{obsd} vs [**2**-Cu(II)$_2$:($^-$OCH$_3$)] for the second event with NaHPNPP (3×10^{-5} M) at 340 nm in anhydrous methanol. The gradient is 0.022 ± 0.013 M^{-1} s^{-1}, intercept = 0.690 ± 0.008 s^{-1}, ^s_spH = 7.4 ± 0.2.

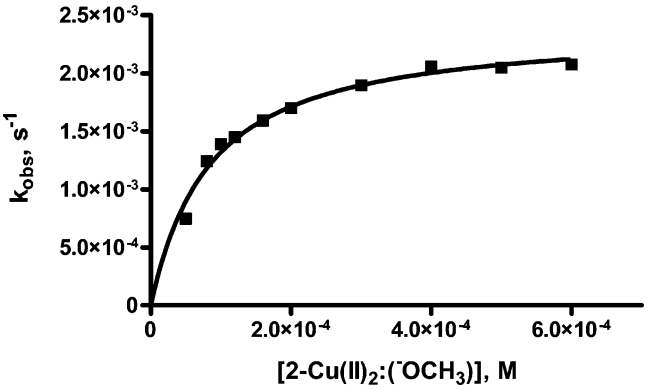

Figure 3. A plot of the first-order rate constants for methanolysis of 0.01 mM **3** vs [**2**-Cu(II)$_2$:($^-$OCH$_3$)]. The line through the data is a fit to the expression in eqs 1, 2 giving a K_M of 0.079 ± 0.018 mM and a k_{cat} of (2.40 ± 0.07) × 10^{-3} s^{-1}; ^s_spH = 7.2 ± 0.2.

In order to investigate the behavior of a DNA derivative which sterically more closely resembles **1** but is far less reactive, we determined the Abs vs time profiles at 340 nm for the reaction of 5×10^{-5} M **4** with varying [**2**-Cu(II)$_2$:($^-$OCH$_3$)] (not shown). This substrate also exhibits the up/down behavior in the UV/vis spectrum as a function of time with a linear dependence on [catalyst] for the first step (k_1 = 8700 ± 300 M^{-1} s^{-1}) and a second step that is independent of [catalyst], k_2 = 0.49 ± 0.03 s^{-1} at an average ^s_spH of 7.1 ± 0.1 (see Table 2 and Supporting Information).

3.1. X-ray Diffraction Structures. Single-crystal X-ray diffraction studies were done on crystals of **2**-Cu(II)$_2$ grown under conditions where (a) the components **2**, Cu(OTf)$_2$, and NaOCH$_3$ were added to dry methanol in a 1:2:1 ratio, followed by diffusion of an ether layer into the methanol solution over a period of about 4 days and (b) the components **2**, Cu(OTf)$_2$, NaOCH$_3$, and the sodium salt of dibenzyl phosphate[37] were added to dry methanol in a 1:2:1:1 ratio, and the solution slowly evaporated in the ambient atmosphere over a period of about 4 days. Shown in Figures 6 and 7 are the structures of **2**-Cu(II)$_2$-($^-$OH)(H$_2$O)(CF$_3$SO$_3^-$)$_3$:0.5CH$_3$CH$_2$OCH$_2$CH$_3$ and **2**-Cu(II)$_2$($^-$-OH)((C$_6$H$_5$CH$_2$O)$_2$PO$_2^-$)(CF$_3$SO$_3^-$)$_2$ without the associated triflate counterions (or CH$_3$CH$_2$OCH$_2$CH$_3$) while selected bond distances and angles are given in Table 3; full details are given in the Supporting Information.

4. Discussion

4.1. X-ray Diffraction Structures. The partial structures shown in Figures 6 and 7, devoid of associated triflate counterions, reveal that both metal ions are five-coordinate and buried rather deeply in the ligand which resembles two tricoordinating "ear-muffs". These impede access to the metal ions from all orientations except those perpendicular to the Cu−Cu axis and distal to the C_3 linking spacer. Apparently there is some flexibility within the ligand that accommodates a variable Cu−Cu distance which ranges from 3.26 to 3.68 Å in passing from **2**-Cu(II)$_2$($^-$OH)(H$_2$O)(CF$_3$SO$_3^-$)$_3$:0.5CH$_3$CH$_2$OCH$_2$CH$_3$ to **2**-Cu(II)$_2$($^-$OH)((C$_6$H$_5$CH$_2$O)$_2$PO$_2^-$)(CF$_3$SO$_3^-$)$_2$. In the former the two Cu(II) ions and coordinated HO$^-$ and OH$_2$ are nearly planar, the intersection angle between the Cu1−($^-$OH)−Cu2 and Cu1(OH$_2$)−Cu2 planes being only 1.1°. The doubly coordinated phosphate diester in **2**-Cu(II)$_2$($^-$OH)((C$_6$H$_5$CH$_2$O)$_2$-PO$_2^-$)(CF$_3$SO$_3^-$)$_2$ has its O3−P1−O4 plane twisted by 68.4° relative to the Cu1−Cu2 axis. The bridging of the diester between the two Cu(II) ions typifies the sort of motif seen in dinuclear complexes where phosphate di- and monoesters are coordinated to the complex.[1,11,27,21,38] It is perhaps important for the catalysis that the O$_3$−P−O$_4$ bond angle in **2**-Cu(II)($^-$-OH)((C$_6$H$_5$CH$_2$O)$_2$PO$_2^-$)(CF$_3$SO$_3^-$)$_2$ is expanded to 118.8° which is similar to that seen with other bridging phosphates in dinuclear Cu(II) complexes[11,38c,d] and may be one reason for the exalted reactivity of the coordinated phosphate diesters in this system; the remaining four O−P−O bond angles are only mildly distorted from tetrahedral, being 105°, 105°, 106°, and 110°. Of note is the fact that the coordinated lyoxide Cu1−O5H−Cu2 is 3.189 Å away from the electrophilic P-center, and when bis-coordinated, the O5H electron pairs are not oriented correctly to assume a nucleophilic role. Thus, it seems likely that if the metal coordinated lyoxide is the nucleophile, it must shed one of the coordinating Cu(II) ions and rotate to allow it to approach the phosphorus.

Given the fact that both crystals were grown from anhydrous methanol solutions (reported to contain 0.002% water or 1.0

(37) Since **1** and **3** react too quickly with methanol in the presence of the catalyst, dibenzyl phosphate was chosen as a nonreactive phosphate for crystal studies.

(38) (a) Feng, G.; Natale, D.; Prabaharan, R.; Mareque-Rivas, J. C.; Williams, N. H. *Angew. Chem., Int. Ed.* **2006**, *45*, 7056. (b) Wall, M.; Hynes, R. C.; Chin, J. *Angew. Chem., Int. Ed. Engl.* **1993**, *32*, 1633. (c) Young, M. J.; Chin, J. *J. Am. Chem. Soc.* **1995**, *117*, 10577.

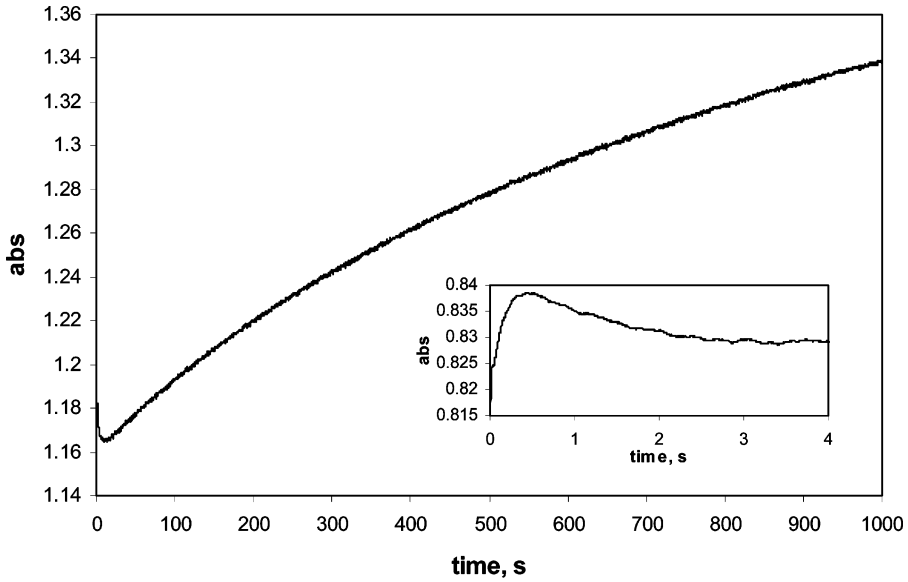

Figure 4. An absorbance vs time profile for the reaction of 0.05 mM **3** in the presence of 0.5 mM **2**-Cu(II)$_2$:($^-$OCH$_3$) showing the three temporally well-defined events; large graph, slow event of product formation followed at 320 nm; inset, the two fast preliminary events followed at 340 nm; T = 25 °C, ^s_spH = 7.1.

Table 2. Various Rate Constants for Binding and Chemical Steps for Substrates **1**, **3**, and **4** Reacting with **2**-Cu(II)$_2$:($^-$OCH$_3$), T = 25 °C

rate constant →/ substrate ↓	k_1 (M^{-1} s^{-1})	k_2 (s^{-1})	k_3 (s^{-1})
1[a]	18 000 ± 700	0.69 ± 0.01	7.0[b]
3[c]	20 200 ± 600	0.53 ± 0.06	(2.40 ± 0.07) × 10^{-3} [d]
4[e]	8700 ± 300	0.49 ± 0.03	N.O.[f]

[a] ^s_spH = 7.4 ± 0.2. [b] Assumed to be at least 10-fold faster than k_2; see text. [c] ^s_spH = 7.1 ± 0.2. [d] Based on saturation data in Figure 3 with K_M = 0.079 ± 0.018 mM, ^s_spH = 7.2 ± 0.2. [e] ^s_spH = 7.1 ± 0.1. [f] Not observed.

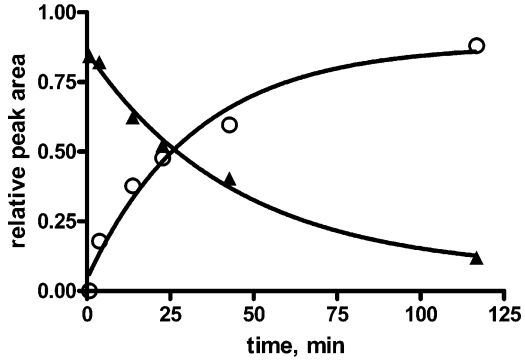

Figure 5. A plot of the relative sums of the integrated intensities of the product (I_{prod}) or substrate (I_3) ESI peak ratios ($I_{prod}/(I_{prod} + I_3)$, ○, and $I_3/(I_{prod} + I_3)$, ▲) as a function of time for the methanolysis reaction of 0.5 mM each of **3** and **2**-Cu(II)$_2$:($^-$OCH$_3$). Lines through the data are NLLSQ fits to a standard exponential model giving k_{prod} = 0.031 ± 0.007 min^{-1} and k_3 = 0.022 ± 0.003 min^{-1}.

mM and used as supplied), it is somewhat surprising to see that neither structure contains methoxide or methanol coordinated to the metal ions, but rather contains only bridging hydroxide or water. The preference for HO^- or OH_2 bridging between the metal ions is not due to the difference in size, as molecular modeling suggests that a methanol or methoxide can occupy the bridging positions without any severe steric interactions. Thus, it appears that the water and hydroxide are preferred due to hydrogen bonded interactions with closely associated $CF_3SO_3^-$ counterions in the crystal. We assume that when in methanol

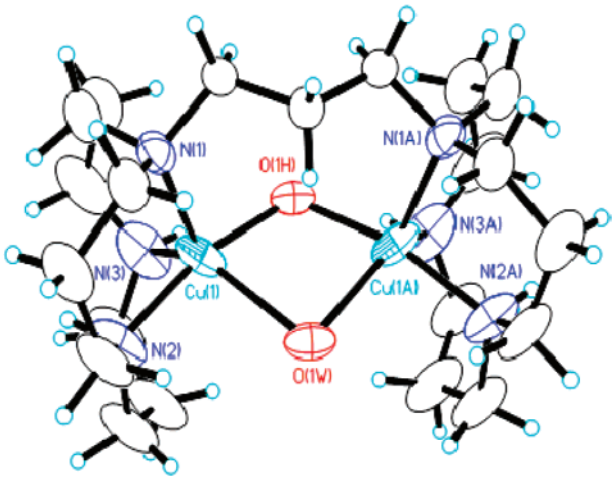

Figure 6. Molecular structure of **2**-Cu(II)$_2$($^-$OH)(H$_2$O)($CF_3SO_3^-$)$_3$:0.5CH_3-$CH_2OCH_2CH_3$ shown as an ORTEP diagram at the 50% probability level; counterions omitted for clarity. Structural details given in the Supporting Information.

solution where the triflate ions can be reasonably well solvated, the bridging positions can be occupied by methoxide and methanol so that, for the reaction of **3**, the product will be a dimethoxy ester as observed for the MS experiments.

4.2. Kinetics. 4.2.1. HPNPP (1) and 2-Cu(II)$_2$:($^-$OCH$_3$). The Abs$_{340}$ nm vs time profile for the reaction of **1** with **2**-Cu(II)$_2$:($^-$OCH$_3$) shown in Figure 1 is biphasic with at least two discernible events. The data in Figure 2, where the kinetics of these two steps are determined by stopped-flow spectrophotometry under pseudo-first-order conditions of excess [**2**-Cu(II)$_2$:($^-$OCH$_3$)] between 0.25 and 1.0 mM, indicate that the rate of the first rapid rise in absorbance is linearly dependent on [**2**-Cu(II)$_2$:($^-$OCH$_3$)], which is consistent with the formation of a **1**:(**2**-Cu(II)$_2$:($^-$OCH$_3$)) complex. At the concentrations of **2**-Cu(II)$_2$:($^-$OCH$_3$) investigated which are at least 5-fold larger than the [**1**], the absorbance change for the first event is constant signifying that essentially all the substrate is bound within the first event. This is consistent with the K_M of 0.079 mM found

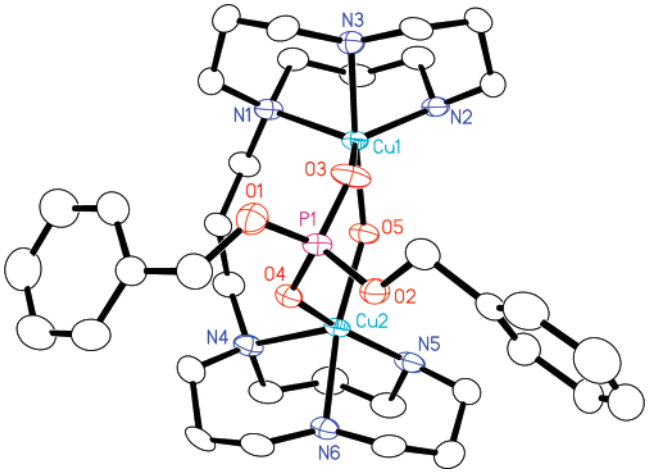

Figure 7. Structure of **2**-Cu(II)$_2$($^-$OH)($C_6H_5CH_2O)_2PO_2^-$)($CF_3SO_3^-$)$_2$ at 50% probability level; counterions omitted for clarity. Details given in the Supporting Information.

with **3** which indicates that these phosphate diester substrates have a high affinity for the catalyst. The second event, which also gives rise to the formation of *p*-nitrophenol product, is independent of [**2**-Cu(II)$_2$:($^-$OCH$_3$)] within experimental uncertainty and so must be a unimolecular process that we suggest arises from a rearrangement of the first-formed **1**:(**2**-Cu(II)$_2$:($^-$OCH$_3$)) complex which places it into a configuration from which an even faster production of *p*-nitrophenol product occurs. Stopped-flow control experiments in the absence of the diesters indicate that neither of these events is attributable to simple dilution of the **2**-Cu(II)$_2$:($^-$OCH$_3$) catalyst. The overall process can be rationalized according to the simplified process presented in Scheme 2 where the first step, having a $k_1 = 18\,000$ M^{-1} s^{-1}, leads to essentially complete formation of the **1**:(**2**-Cu(II)$_2$:($^-$OCH$_3$)) complex, while the second rearrangement step has an average pseudo-first-order rate constant of $k_2 = 0.69$ s^{-1} at ^s_spH = 7.4 ± 0.2. The subsequent product forming step, k_3 in Scheme 1, must be faster than the second step (we have assumed by at least 10-fold) which accounts for the apparent rise in absorbance for the k_2 step relative to the cases with the slower reacting phosphates described below.

4.2.2. Methyl *p*-Nitrophenyl Phosphate (3) and 2-Cu(II)$_2$:($^-$OCH$_3$). Since the second event with **1** and **2**-Cu(II)$_2$:($^-$OCH$_3$), which we attribute to an intramolecular rearrangement, appears to be superimposed on a subsequent fast chemical process that forms the observable *p*-nitrophenol product, we switched to the DNA model **3** where the release of *p*-nitrophenol is far slower than that with **1**.[23,35] When the kinetics of production of *p*-nitrophenol are monitored by normal UV/vis spectrophotometry at 320 nm under pseudo-first-order conditions as a function of [**2**-Cu(II)$_2$:($^-$OCH$_3$)] at ^s_spH = 7.2 ± 0.2, one observes the saturation kinetic plot shown in Figure 3 which can be analyzed with eqs 1 and 2 to yield a K_M of 0.079 ± 0.018 mM and a k_{cat} of (2.40 ± 0.07) × 10^{-3} s^{-1}. The numerical value of K_M indicates that the binding of **3**, and presumably closely related phosphate diesters such as **1** and **4**, is strong. Based on the above analysis with **1** we expect three observed events for **3**, with the first two being attributed to binding and rearrangement and the third to a slower chemical event that liberates the *p*-nitrophenol. Indeed, these expectations for the first two fast events are borne out by the data shown in Figure 4 in which the insert reveals a rapid rise/fall behavior followed at 340 nm. When these two events are followed at ^s_spH = 7.2 ± 0.2 by stopped-flow spectrophotometry at 0.25 mM < [**2**-Cu(II):($^-$OCH$_3$)] < 1.0 mM (all values being above the K_M value so that the binding should be essentially saturated), one determines that $k_1 = 20\,200$ ± 600 M^{-1} s^{-1} and $k_2 = 0.53 \pm 0.06$ s^{-1}.

The observed kinetic behavior for substrate **4**, which is far less reactive than **1** or **3** but sterically similar to the structure of **1**, closely parallels that of **3** for the first two binding steps where the first event was determined to be first order in [catalyst] with $k_1 = 8700 \pm 300$ M^{-1} s^{-1} while the second step was independent of [catalyst], k_2 being 0.49 ± 0.03 s^{-1} at an average ^s_spH of 7.1 ± 0.1. The k_3 step that would pertain to the release of *p*-chlorophenol is observed to be far slower than in the case of **3** and was not followed for this substrate.

4.3. Electrospray MS Measurements. In order to probe the nature of the products of the reaction, the ESI mass spectra of aliquots removed from a methanol solution that was 0.5 mM in each of **3** and **2**-Cu(II)$_2$:($^-$OCH$_3$) were determined as a function of time. These are conditions where all the phosphate material should be bound 1:1 to the **2**-Cu(II)$_2$ complex. The ratios of the sums of the total integrated intensity of all the major peaks containing product $(CH_3O)_2PO_2^-$, (I_{prod}), and all those containing the starting material **3**, (I_3) vs ($I_{prod} + I_3$), were plotted as a function of time as shown in Figure 5. At the end of the reaction, all the **3** was consumed and the only peaks that were observed were those attributable to **2**-Cu(II)$_2$:(OTf^-)$_2$(($CH_3O)_2PO_2^-$) and **2**-Cu(II)$_2$:(OTf^-)(($CH_3O)_2PO_2^-$)$_2$.

4.4. General Mechanistic and Energetic Considerations of the Catalysis. The observed events for all three substrates are consistent with the simplified process shown in Schemes 1 and 2. The major difference relates to the magnitude of the rate constants for the k_3 process which vary from ≫0.7 s^{-1} for HPNPP to (2.40 ± 0.07) × 10^{-3} s^{-1} for **3** and is too slow to measure within a reasonable time with **4**. The clearest case for three temporally well-separated events is that of the catalyzed methanolysis of **3** where there is evidence consistent with separate bimolecular catalyst:substrate binding and intramolecular rearrangement events, followed by the slower chemical step for the production of *p*-nitrophenol. The data in Table 2 indicate that the two events that precede the chemical step have very similar rate constants for all substrates which seems most consistent with more-or-less common binding processes. The value for the k_1 step seems small for ligand exchange on Cu(II) complexes, which in some cases can be very high ((2−20) × 10^8 M^{-1} s^{-1}).[39] However the rates of binding to M(II) complexes in general are known[40] to be highly sensitive to crowding effects such as is the case here. The compactness of the **2**-Cu(II)$_2$-($^-$OH)(H_2O)($CF_3SO_3^-$)$_3$ structure shown in Figure 7 suggests that substrate coordination to the Cu(II) ion(s) cannot occur by an associative process but rather requires that the complex should open up, probably by an equilibrium dissociation of one of the Cu−O(H$_2$)−Cu bonds, to reveal a four-coordinate Cu(II) with an open site to which the phosphate can then bind. If the equilibrium concentration of the open form is small, as expected, then the overall rate constant for the association of

(39) Tobe, M. L.; Burgess, J. *Inorganic Reaction Mechanisms*; Addison Wesley Longman Ltd.: New York, 1999; pp 271−333,
(40) (a) Dukes, G. R.; Margerum, D. W. *Inorg. Chem.* **1972**, *11*, 2952. (b) Pitteri, B.; Marangoni, G.; Viseutin, F. V.; Cattalini, L.; Bobbo, T. *Polyhedron* **1998**, *17*, 475.

Scheme 2 [a]

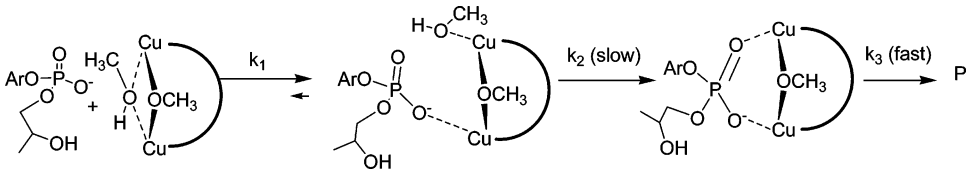

[a] Proposed reaction sequence for HPNPP (**1**) and **2**-Cu(II)$_2$:($^-$OCH$_3$); charges omitted for clarity.

Table 3. Selected Bond Distances and Angles for **2**-Cu(II)$_2$($^-$OH)(H$_2$O)(CF$_3$SO$_3^-$)$_3$:0.5CH$_3$CH$_2$OCH$_2$CH$_3$ and **2**-Cu(II)$_2$($^-$OH)(C$_6$H$_5$CH$_2$O)$_2$PO$_2^-$)(CF$_3$SO$_3^-$)$_2$ as Determined from X-ray Diffraction[a]

parameter	**2**-Cu(II)($^-$OH)(H$_2$O)	**2**-Cu(II)($^-$OH)((C$_6$H$_5$CH$_2$O)$_2$PO$_2^-$)
Cu−Cu (Å)	3.260	3.680
Cu1−OH (Å)	1.897	1.944
Cu2−OH (Å)	1.987	1.945
Cu1−O(H$_2$); Cu2−O(H$_2$) (Å)	2.342, 2.342	
Cu1−OP; Cu2−OP (Å)		2.022; 1.986
O5−P (Å)		3.189
∠Cu1−OH−Cu2 (deg)	118.46	140.44
∠Cu1−OH$_2$−Cu2 (deg)	88.22	
∠OH−Cu1−OH$_2$; OH−Cu2−OH$_2$ (deg)	76.66; 76.66	
∠OH−Cu1−OP; OH−Cu2−OP (deg)		89.39; 89.00
∠O$_3$−P−O$_4$ (deg)		118.83

[a] For a complete listing of band angles and distances as well as atomic coordinates, see the Supporting Information.

phosphate will be reduced accounting for the 9 000−20 000 M^{-1} s^{-1} values for k_1 seen here. The second step is consistent with an intramolecular rearrangement, probably to form a doubly coordinated phosphate with a structure similar to what is shown in Figure 7 with a coordinated dibenzyl phosphate. The slowness of this step can also be attributed to the tight steric requirements that may impede the required dissociation of the bound solvent from the second Cu(II) prior to double coordination of the phosphate.

The effectiveness of the catalysis of the chemical steps with **1** and **3** can be measured in several ways. First, one could compare the effective second-order rate constant for the catalytic reaction with **3** (given as $k_{cat}/K_M = 2.4 \times 10^{-3}$ $s^{-1}/7.9 \times 10^{-5}$ M = 30 M^{-1} s^{-1}) with that for the methoxide reaction (7.9×10^{-7} M^{-1} s^{-1}); by this measure, the acceleration imbued by **2**-Cu(II)$_2$:($^-$OCH$_3$) is 3.8×10^7-fold. This is similar to the catalysis afforded for methanolysis of **3** by **2**-Zn(II)$_2$:($^-$OCH$_3$),[23] where $k_{cat}/K_M = (4.1 \pm 0.3) \times 10^{-2}$ $s^{-1}/(0.37 \pm 0.07)$ mM = 110 M^{-1} s^{-1}, the acceleration relative to the methoxide reaction being 1.4×10^8. In the case of the reactions with the RNA model **1**, the chemical step of production of *p*-nitrophenol is far faster than the limiting rearrangement process, so the calculation leads only to a lower limit for the acceleration. With **2**-Cu(II)$_2$:($^-$OCH$_3$), assuming that the K_M constant can be approximated by that found for **3** and that the chemical step is at least 10-fold faster than the rearrangement step (~7 s^{-1}), the acceleration is 3.5×10^7-fold (calculated as 7 $s^{-1}/7.9 \times 10^{-5}$ M/2.56 $\times 10^{-3}$ M^{-1} s^{-1}). Even if one uses the rate constant determined by the rate-limiting second rearrangement step (0.7 s^{-1}), the acceleration is 3.5×10^6. Alternatively, if the first binding step of the substrate to the complex is rate limiting at 18 000 M^{-1} s^{-1}, the acceleration relative to the methoxide reaction is computed as 7.0×10^6-fold. Comparison with the **2**-Zn(II)$_2$:($^-$OCH$_3$) catalyst is also complicated by the fact that the latter does not show Michaelis−Mentin kinetics, but rather second-order kinetics with a rate constant of 275 000 M^{-1} s^{-1} where the rate-limiting step was proposed[23] to be substrate binding.[41] Using this number, the overall catalysis by the Zn(II)$_2$ complex is 1.1×10^8-fold.

A second way to compare the catalyst efficacy is to measure the rate acceleration relative to the methoxide reaction at the ^s_spH where the catalyst is operative (7.2 in the case of **2**-Cu(II)$_2$:($^-$OCH$_3$), 9.5 in the case of **2**-Zn(II)$_2$:($^-$OCH$_3$)).[42] This artificially enhances the computed catalysis for systems that operate at lower "pH" values but is a generally accepted method for enzymatic reactions where the efficacy of the catalyzed process is analyzed at neutral pH's where the enzymes operate. In this case, at ^s_spH 7.2 (or 9.5) the methoxide reactions of **1** and **3** would have first-order rate constants of 6.9×10^{-13} (1.4×10^{-10}) s^{-1} and 2.1×10^{-16} (4.3×10^{-14}) s^{-1}, respectively. For the **2**-Cu(II)$_2$ catalyst, where the rate-limiting step is the intramolecular rearrangement with **1** or **3** having a rate constant of ~0.7 s^{-1}, the respective accelerations are about 10^{12}- and 10^{13}-fold. For a solution containing 1 mM of the **2**-Zn(II)$_2$ catalyst operating at ^s_spH 9.5, the acceleration of cleavage of **1** is 2×10^{12}-fold, while the acceleration exhibited by **2**-Zn(II)$_2$:($^-$OCH$_3$)-bound **3** (which decomposes with a pseudo-first-order rate constant of 4.1×10^{-2} s^{-1})[23] is also about 10^{12}.

A recent analysis of the reaction of a dinuclear Zn(II) complex (**5**) reacting with HPNPP[43] presents a third and thermodynami-

(41) A referee has suggested that there is good evidence from other studies (see ref 17) with a dinuclear Zn(II) complex (**5**) in aqueous solution that the binding involves the nonionized form of the catalyst (Zn(II)$_2$:H$_2$O) and the 2-hydroxy deprotonated dianionic form of HPNPP rather than the Zn(II)$_2$:$^-$OH form of the catalyst and the protonated 2-OH form of HPNPP which we favor on the basis of our studies. While it is true that these two possibilities are kinetically equivalent and cannot be distinguished on the basis of catalytic studies with **5** in water due to its relatively low activity, the available results we have with **2**-Cu(II)$_2$:($^-$OCH$_3$) or **2**-Zn(II)$_2$:($^-$OCH$_3$) reacting with HPNPP in methanol quickly rule out the former possibility. The pK_a for deprotonation of the 2-HO group of HPNPP in methanol should be at least as large or greater than that of methanol (K_w/[MeOH] = $10^{-16.77}$/30) or ^s_spK_a = 18.2. At a ^s_spH of 7.2 or 9.5 where the 2-Cu(II) and **2**-Zn(II) are operative, the [HPNPP^{2-}] would be one part in 10^{11} and one part in $10^{8.7}$ respectively. Since the second-order rate constants for binding of the HPNPP substrate, in whatever form, by the **2**-Cu(II) and **2**-Zn(II) catalysts are observed to be 18 000 and 275 000 M^{-1} s^{-1}, respectively, the reactions would have to exceed the diffusion limit of 10^{10} M^{-1} s^{-1} by at least 10^4 if the dianionic form of the substrate was the active one.

(42) Since the autoprotolysis constant of methanol is $10^{-16.77}$, at ^s_spH 7.2 or 9.5 the [CH$_3$O$^-$] is 2.69×10^{-10} or 5.4×10^{-8} M.

Scheme 3

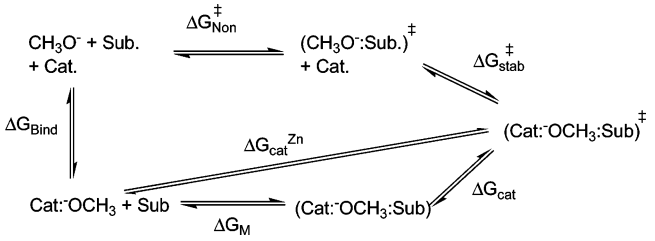

cally explicit way of comparing the lyoxide and complex-catalyzed reactions by analyzing the transition state energetics and the stabilization of the lyoxide:substrate transition state through its binding to the catalyst.[44] Scheme 3 gives a thermodynamic cycle describing both the methoxide reaction and the **2**-M(II)$_2$:($^-$OCH$_3$) complex promoted reaction. Given in eq 3 is the expression for computing the free energy of binding of the transition state for the catalyst promoted reaction relative to the methoxide reaction ($\Delta G^{\ddagger}_{stab.}$). The term "methoxide reaction" which is given a short-hand designation of (CH$_3$O$^-$:Sub.)‡ in Scheme 3 refers to both of the reactions with **1** and **3** where methoxide acts as a base or a nucleophile. In eq 4 is the free energy calculation specific for the reaction with HPNPP and **2**-Zn(II)$_2$:($^-$OCH$_3$) which does not show saturation kinetics but does show an overall second-order reaction with a first-order dependence on [catalyst]. The terms in eqs 3, 4 are calculated from the following: (a) k_{cat}/K_M from the saturation curve depicted in Figure 3 or that given in ref 23 for the reaction of **3** with the Zn(II) complex; (b) K_a/K_w can be readily interpreted as the binding constant of methoxide to the dinuclear complex, where K_a refers to the first acid dissociation constant for the formation of **2**-Cu(II)$_2$:($^-$OCH$_3$) or **2**-Zn(II)$_2$:($^-$OCH$_3$) and K_w is the autoprotolysis constant for methanol ($10^{-16.77}$); and (c) k_{OCH_3} is the second-order rate constant for the methoxide reactions in the absence of complex. Listed in Table 4 are the various constants for the relevant terms in eq 3 for the reaction with **3** and **1** with the **2**-Cu(II)$_2$ catalyst and **3** with the **2**-Zn(II)$_2$ catalyst and those in eq 4 for the reaction of HPNPP with the **2**-Zn(II)$_2$ catalyst.

$$\Delta G^{\ddagger}_{stab} = (\Delta G_{Bind} + \Delta G_M + \Delta G_{cat}) - \Delta G^{\ddagger}_{Non} = - RT \ln\left[\frac{(k_{cat}/K_M)(K_a/K_w)}{k_{OCH_3}}\right] \quad (3)$$

In Scheme 3, ΔG_{bind}, ΔG_{cat}, and $\Delta G^{\ddagger}_{Non}$ are the respective free energies for (1) binding of methoxide to the catalyst; (2) the activation energy for unimolecular reaction of the Cat:$^-$OCH$_3$:Sub. complex; and (3) the activation energy for the reaction of methoxide alone with substrate. ΔG_M is the free energy for association of the substrate and Cat:$^-$OCH$_3$ complex. In eq 4, ΔG^{Zn}_{cat} is the free energy for the second-order reaction of the Cat:$^-$OCH$_3$ complex with substrate, the associated rate constant being defined as k_1^{obsd}.

$$\Delta G^{\ddagger}_{stab} = (\Delta G_{Bind} + \Delta G^{Zn}_{cat}) - \Delta G^{\ddagger}_{Non} = - RT \ln\left[\frac{(k_1{}^{obsd})(K_a/K_w)}{k_{OCH_3}}\right] \quad (4)$$

As described above, we do not see saturation kinetics for HPNPP binding and reaction with either catalyst, but for **2**-Cu(II)$_2$:($^-$OCH$_3$) we can estimate a lower limit for the k_{cat} term as 0.7 s^{-1} from the rate-limiting intramolecular rearrangement and estimate the K_M term as 7.9×10^{-5} M based on the one found for **3** (*vide supra*). In reality the k_{cat} term for the chemical step must be much greater which will actually give a larger stabilization of ΔG (an extra -1.4 kcal for each factor of 10 in rate constant at 25 °C). For **2**-Zn(II)$_2$:($^-$OCH$_3$) we see only second-order kinetics for the reaction of catalyst and HPNPP substrate to produce *p*-nitrophenol, the limiting rate constant (k_1^{obsd}) being 275 000 M^{-1} s^{-1} which we have interpreted as being due to the binding of HPNPP and catalyst. Using these values, the lower limit for computed stabilization of the TS for the intramolecular transesterification of HPNPP with CH$_3$O$^-$ bound by the Cu(II)$_2$ and Zn(II)$_2$ catalysts are -22.6 and -21.0 kcal/mol, while those for the reaction of **3** promoted by the same two catalysts are -24.0 and -21.1 kcal/mol. These are very large energy reductions for two dinuclear catalysts promoting two different reactions where one involves a methoxide (either metal-coordinated or free) acting as a base followed by an intramolecular cylcization and subsequent formation of product, while the other reaction involves methoxide acting as a nucleophile on P.

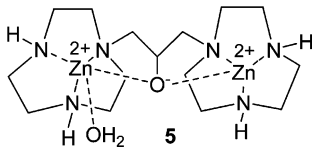

5

The large TS binding energies of the **2**-M(II)$_2$ catalysts for **1** and **3** in methanol, while approximate given the assumptions, invite comparison with the value of -9.6 kcal/mol afforded for the cleavage of HPNPP by dinuclear Zn(II) complex **5** in water.[43] To our knowledge there are no such free energy comparisons possible from literature examples for the catalyzed cleavage of DNA models, presumably probably because these reactions are extremely slow in water unless catalyzed efficiently as is the case here in methanol. The combination of these two specific dinuclear complexes (whether Zn(II) or Cu(II) containing) and a medium effect engendered by the methanol, provides rate enhancements exceeding anything reported in water so far. Previously[23] we attributed this medium effect in the light alcohol solvents to a reduced dielectric constant that increases the potential energy of attraction between oppositely charged ions of the sort involved in metal-catalyzed reactions of anionic substrates. In addition, a lower polarity medium is well-known to promote reactions where charge is dispersed in the TS. The application of eqs 3, 4 allows one to assess the energetic consequences of the medium effect on the various rate and equilibrium steps shown in Scheme 3 for different catalytic systems as in eq 5

$$\Delta\Delta G^{\ddagger}_{stab} = -RT \ln\left\{\left(\frac{(k_{cat}/K_M)^{MeOH}}{(k_{cat}/K_M)^{HOH}}\right)\left(\frac{[K_a/K_w]^{MeOH}}{[K_a/K_w]^{HOH}}\right)\left(\frac{(k_{OH})^{HOH}}{(k_{OMe})^{MeOH}}\right)\right\} \quad (5)$$

(43) O'Donoghue, A. M.; Pyun, S. Y; Yang, M.-Y.; Morrow, J. R.; Richard, J. P. *J. Am. Chem. Soc.* **2006**, *128*, 1615.
(44) Wolfenden, R. *Nature* **1969**, *223*, 704.

Table 4. Kinetic Parameters for **2**-M(II)$_2$:($^-$OCH$_3$) and Methoxide Ion Catalyzed Cleavage of **3** and HPNPP (**1**) at 25 °C in Methanol

parameter	**3** (Cu(II))	**3** (Zn(II))	HPNPP (Cu(II))	HPNPP (Zn(II))
k_{OCH_3} (M^{-1} s^{-1})	7.9×10^{-7} [a]	7.9×10^{-7} [a]	2.56×10^{-3} [b]	2.56×10^{-3} [b]
K_M (M)	7.9×10^{-5} [c]	3.7×10^{-4} [a]	7.9×10^{-5} [d]	−
k_{cat}/K_M (M^{-1} s^{-1})	30	110[a]	9×10^3	275 000[e]
K_a/K_w (M^{-1})	10^{10} [f]	2.3×10^7 [f]	10^{10} [f]	2.3×10^7 [f]
$(k_{cat}/K_M)(K_a/K_w)$ (M^{-2} s^{-1})	30×10^{10}	2.5×10^9	9×10^{13}	6.3×10^{12}
$\Delta G^{\ddagger}_{stab}$ (kcal/mol)	−24.0	−21.1	≤− 22.6	≤− 21.0

[a] From ref 23. [b] From ref 33. [c] From data in Figure 3. [d] K_M for HPNPP assumed to be the same as that determined for **3**. [e] Given as second-order rate constant observed in ref 23 for the reaction of Zn(II) catalyst with HPNPP (k_1^{obsd}) [f] K_a from half neutralization of **2**-Cu(II)$_2$:($^-$OCH$_3$) and **2**-Zn(II)$_2$:($^-$OCH$_3$) by adding 0.5 equiv of acid to the **2**-M(II)$_2$:($^-$OCH$_3$) complex, $^{s}_{s}pK_a = 6.77$ and 9.41, respectively.

Table 5. Computed $\Delta\Delta G^{\ddagger}_{stab}$ Afforded from Each of the Ratios of Constants Given in Eq 5 for the Reactions of Various Systems in Promoting the Cyclization of HPNPP (**1**) at 25 °C

catalyst comparison↓	$[-RT\ln\{(k_{cat}/K_m)^{MeOH}/(k_{cat}/K_m)^{HOH}\}]$ (kcal/mol)[a]	$\{-RT\ln([K_a/K_w]^{MeOH}/[K_a/K_w]^{HOH})\}$ (kcal/mol)	$[-RT\ln\{(k_{OH})^{HOH}/(k_{OMe})^{MeOH}\}]$ (kcal/mol)	total $\Delta\Delta G^{\ddagger}_{stab}$methanol vs water (kcal/mol)
2-Zn(II)$_2$ in MeOH vs **5** in water	−7.6	−1.6	−2.2	−11.4
2-Cu(II)$_2$ in MeOH vs **5** in water	−5.6	−5.2	−2.2	−13

[a] The k_{cat}/K_M term is given as the second-order rate constant for **2**-Zn(II)$_2$ promoted cylcization of **1** (2.75×10^5 M^{-1} s^{-1}), while that for **2**-Cu(II)$_2$ is given as 0.7 s^{-1}/7.9×10^{-5} M: the reported rate constant for the reaction of **5** with HPNPP in water is 0.71 M^{-1} s^{-1} (ref 43).

where the k_{cat}/K_M term can be replaced by the apparent second-order rate constant for the catalyst reacting with HPNPP or **3**. Ideally one would like to compare the same catalyst in water and methanol, but this is not possible at present. Nevertheless, the energy differences ($\Delta\Delta G^{\neq}_{stab}$) shown in Table 5 shed light on which of the components contributes most to the observed increase in catalysis in moving between the two systems. For example, the K_a/K_w term has a value of 1.43×10^6 M^{-1} in water with the Zn(II) catalyst **5**,[43] 2.3×10^7 M^{-1} in methanol with **2**-Zn(II)$_2$, and 1×10^{10} M^{-1} in methanol with **2**-Cu(II)$_2$. Although the autoprotolysis constant for methanol ($K_w = 10^{-16.77}$) is lower than that of water, this only leads to an increase in the K_a/K_w term if the $^{s}_{s}pK_a^{methanol} < (pK_a^{water} + 2.77)$. The $^{s}_{s}pK_a$ for ionization of **2**-Zn(II):(HOCH$_3$) is 9.41, while the pK_a for **5** in water is 7.8−8.0[43] such that the respective and K_a/K_w ratios for **5** and **2**-Zn(II) differ by a factor of 16. This term contributes −1.64 kcal/mol to the stabilization of the TS ($\Delta\Delta G^{\ddagger}_{stab}$) for the reaction of **2**-Zn(II) in methanol vs **5** in water but a more substantial −5.24 kcal/mol for the **2**-Cu(II) complex in methanol because its $^{s}_{s}pK_a$ of 6.77 is nearly 3 units lower than that of the Zn(II) complex.

The difference between the k_{OR} values for reaction of **1** with hydroxide in water (9.9×10^{-2} M^{-1} s^{-1})[43] and methoxide in methanol (2.56×10^{-3} M^{-1} s^{-1}) contributes −2.2 kcal/mol to the overall $\Delta\Delta G^{\ddagger}_{stab}$. However, the analysis shows that the major part of the $\Delta\Delta G^{\ddagger}$ stabilization in the case of the **2**-Zn(II)$_2$ complex results from the apparent second-order rate constant (k_{cat}/K_M) for the reaction which is 3.9×10^5 times larger than that seen in the case of **5** in water. The analogous value for **2**-Cu(II)$_2$ is 1.3×10^4 times larger and, thus, contributes roughly as much as its K_a/K_w term to the overall $\Delta\Delta G^{\ddagger}_{stab}$ for the reaction.

5. Conclusions

In the above we have provided structural data for two **2**-Cu(II)$_2$ complexes where the central coppers are bridged by HO$^-$, H$_2$O, and HO$^-$, (PhCH$_2$O)$_2$PO$_2^-$ (Figure 7, respectively). These are germane to the solution forms of the resting catalyst in methanol where methoxide seems to be the active base or nucleophile and to the state in which the reactive phosphate diesters **1** and **3** studied here might be bound prior to their cleavage. The kinetic studies of **2**-Cu(II)$_2$:$^-$OCH$_3$ with substrates **1**, **3**, and **4** demonstrate that all have two fast steps that are interpreted as substrate binding to one of the Cu(II) centers, followed by an intramolecular rearrangement to form a putative double Cu(II) coordinated phosphate diester analogous to what is shown in Figure 7. For two of these systems, **1** and **3**, there is a chemical event that leads to the production of *p*-nitrophenol which is markedly accelerated relative to the background reaction promoted by methoxide. In fact the acceleration of the chemical step in the reaction of **1** is so effective that the rate-limiting steps become those of substrate binding and positioning.

The accelerations afforded to the cleavage of **1** and transesterification of **3** by **2**-Cu(II)$_2$:($^-$OCH$_3$) catalyst are among the fastest reported to date, the only faster ones being with our previously reported[23] **2**-Zn(II)$_2$:($^-$OCH$_3$) catalyst also in methanol. An analysis of the free energy of binding of the **2**-Cu(II)$_2$ and **2**-Zn(II)$_2$ catalysts to the TS for the intramolecular cyclization of **1** and the phosphoryl transfer process of **3** indicates that these two dinuclear systems exhibit similar values of −21 to −24 kcal/mol which is significantly greater than what has been heretofore reported for a dinuclear system catalyzing three analogous phorphoryl cyclizations in water (−7.2 to −9.6 kcal/mol).[43] A detailed analysis partitions the origins of the differences in the free energies of stabilization of the methanol/**2** system vs a water/**5** system into three main terms that are responsible for the $\Delta\Delta G^{\ddagger}_{stab}$ where the main contributions arise from the increased catalytic constants (k_{cat}/K_M).

The results from this study reinforce our previous contentions[23] that the combination of the dinuclear catalysts and an important medium effect contribute greatly to the acceleration of the cleavage of phosphate diesters and that such a combination may fulfill a key role in related enzymatic processes.

Acknowledgment. The authors gratefully acknowledge the Natural Engineering Sciences and Research Council of Canada, the Canada Foundation for Innovation, The Canada Council for the Arts, and Queen's University for financial support of this work. They are also grateful to Dr. Ruiyao Wang for determining the X-ray diffraction structures of the **2**-Cu(II)$_2$ complexes.

In addition C.T.L. acknowledges NSERC Canada for a postgraduate PGS-M scholarship.

Supporting Information Available: Tables of pseudo-first-order rate constants for reactions of **1**, **3**, and **4** with **2**-$Cu(II)_2$:($^{-}OCH_3$); mass spectra at three different reaction times for **3** with equimolar **2**-$Cu(II)_2$:($^{-}OCH_3$); structural reports and CIF files for **2**-$Cu(II)_2(^{-}OH)(C_6H_5CH_2O)_2PO_2^{-})(CF_3SO_3^{-})_2$ and **2**-$Cu(II)_2(^{-}OH)(H_2O)(CF_3SO_3^{-})_3$:$0.5CH_3CH_2OCH_2CH_3$. This material is available free of charge via the Internet at http://pubs.acs.org.

JA073780L